

Measurement of subpicosecond electron pulses

Hung-chi Lihn,* Pamela Kung, Chitrlada Settakorn, and Helmut Wiedemann

Applied Physics Department and Stanford Linear Accelerator Center, Stanford University, Stanford, California 94309

David Bocek

Physics Department and Stanford Linear Accelerator Center, Stanford University, Stanford, California 94309

(Received 30 August 1995)

A bunch-length measuring method has been developed to measure the subpicosecond electron pulses generated at the Stanford University Short Intense Electron Source (SUNSHINE) facility. This method utilizes a far-infrared Michelson interferometer to measure coherent transition radiation emitted at wavelengths longer than or equal to the bunch length via optical autocorrelation. To analyze the measurement, a simple and systematic way has also been developed, which considers interference effects on the interferogram caused by the beam splitter; hence the electron bunch length can be easily obtained from the measurement. This simple, low-cost, frequency-resolved autocorrelation method demonstrates subpicosecond resolving power that cannot be achieved by existing time-resolved methods. [S1063-651X(96)05906-5]

PACS number(s): 29.17.+w, 07.60.-j, 29.27.Fh, 41.75.Ht.

I. INTRODUCTION

In recent years, the reduction of electron bunch length has become an interesting aspect in the development of particle accelerators. Its progress greatly affects the design of next-generation synchrotron light sources, future linear colliders, free-electron lasers, and high-intensity coherent far-infrared light sources. For example, the proposed future machines such as future linear colliders and single-pass x-ray free-electron lasers demand the electron bunch length to be less than 0.1 ps, which is not even presently measurable. Hence, a bunch-length measuring system capable of characterizing subpicosecond pulses will provide a powerful tool to measure such progress.

It is intuitive to use a time-resolved method to measure the electron bunch length, which resolves the beam-generated signal in the time domain. However, when the bunch length is in the subpicosecond regime, it is beyond the resolution of time-resolved methods developed so far. Nevertheless, the complexity and the cost of hardware for fast time-resolved methods, such as a streak camera, increase to a great extent as the resolution approaches one picosecond. It is necessary therefore to develop an alternative bunch-length measuring technique with subpicosecond resolving power.

As an alternative, a frequency-resolved technique extracts the frequency content of a beam-generated signal. From this frequency information, the particle distribution can be deduced. Unlike time-resolved techniques, this does not require fast processing speed and complex hardware. Since the necessary broad bandwidth required for short pulses can be achieved by optical methods, a subpicosecond time resolution can be obtained. This is a well known technique in the characterization of femtosecond laser pulses [1] and has been suggested for subpicosecond bunch-length measurement [2]. The method utilizes a far-infrared Michelson interferometer to measure coherent transition radiation emitted at wave-

lengths longer than or equal to the bunch length via optical autocorrelation. The bunch length can be determined by analyzing the measured frequency information.

At the SUNSHINE facility, we have developed an alternative bunch-length measuring system based on this frequency-resolved method. Using subpicosecond electron pulses generated at SUNSHINE [3,4], we have verified this technique [4,5] and developed it into a simple, low-cost instrument for subpicosecond bunch-length measurement. In this paper, we describe the principle of this autocorrelation technique, the analysis and interpretation of bunch-length measurements, and the experimental results.

II. AUTOCORRELATION BUNCH-LENGTH MEASURING METHOD

This frequency-resolved method uses a far-infrared Michelson interferometer to measure the spectrum of coherent transition radiation via optical autocorrelation. Coherent transition radiation emitted by electron pulses carries the information of bunch distribution in its frequency content. By analyzing the frequency information, the bunch length can be derived.

A. Coherent transition radiation

Transition radiation is generated when an electron passes the interface of two media of different dielectric constants [6]. The spectral distribution is determined by the frequency dependence of the dielectric constants of the media. For a vacuum-metal interface, the spectrum of transition radiation is approximately constant in the far-infrared regime due to the almost perfect conductivity of the metal, and the angular spectral energy for the case of normal incidence can be expressed as [6]

$$\frac{d^2\mathcal{E}}{d\omega d\Omega} = \frac{e^2\beta^2}{\pi^2 c} \frac{\sin^2\theta}{(1-\beta^2\cos^2\theta)^2}, \quad (1)$$

where θ is the angle between the radiation and the electron

*Electronic address: Wiedemann@SSRL01.SLAC.Stanford.edu

direction, and β the ratio of the speed of the electron to that of light. For a relativistic electron, this distribution has a zero at $\theta=0$ and reaches maximum at $\theta\sim 1/\gamma$, where γ is the Lorentz factor.

When a bunch of N electrons passes the interface, the resulting total electric field at the observation point is the superposition of the one emitted from each electron. If the observation point is far from the interface, the total intensity at wavelength λ , using far-field approximation, can be expressed as [7]

$$I_{\text{total}}(\lambda) = N[1 + (N-1)f(\lambda)]I_e(\lambda), \quad (2)$$

where $I_e(\lambda)$ is the intensity of transition radiation emitted by an electron at wavelength λ . In the far-infrared regime, $I_e(\lambda)$ is constant. The form factor $f(\lambda)$ is given by the three-dimensional Fourier transform of the normalized bunch distribution $W(\mathbf{r})$ [$\int W(\mathbf{r})d\mathbf{r}=1$]

$$f(\lambda) = \left| \int W(\mathbf{r}) e^{i2\pi(\hat{\mathbf{n}} \cdot \mathbf{r})/\lambda} d\mathbf{r} \right|^2, \quad (3)$$

where $\hat{\mathbf{n}}$ is the unit vector directed from the center of the bunch to the observation point and \mathbf{r} is the position vector of an electron relative to its bunch center. If the radiation is observed in the forward direction (which is defined as the unit vector $\hat{\mathbf{z}}$; $\hat{\mathbf{n}}\parallel\hat{\mathbf{z}}$) from a transversely symmetric beam with rectangular longitudinal distribution, the form factor $f(\lambda)$ is the square of a sinc function, which is independent of the transverse bunch distribution. Similarly, for a Gaussian longitudinal distribution, $f(\lambda)$ is also Gaussian [7]. For wavelengths longer than the bunch length, the form factor approaches unity, and the total radiation intensity is coherent [$I_{\text{total}}(\lambda)\propto N^2$]. On the other hand, for wavelengths shorter than the bunch length, the form factor reduces to zero, and the radiation becomes incoherent [$I_{\text{total}}(\lambda)\propto N$]. The coherent radiation has N times more intensity than the incoherent one. Hence not only does coherent transition radiation carry the bunch distribution information, it is also easier to detect than its incoherent counterpart.

It is worth noticing that transition radiation does not produce radiation in the forward direction [$\theta = \cos^{-1}(\hat{\mathbf{n}} \cdot \hat{\mathbf{z}}) = 0$]. Hence in order to use transition radiation to measure the bunch length, it is necessary to observe the radiation in an off-axis direction ($\theta \neq 0$). In the case of an off-axis observation, the transverse bunch distribution will contribute to the form factor even for a transversely symmetric beam. Minimizing such a contribution becomes important for clean subpicosecond bunch-length measurements. For example, the form factor for a cylindrical beam of radius ρ and length l , when observed at an angle θ (i.e., $\hat{\mathbf{n}} \cdot \hat{\mathbf{z}} = \cos\theta$), is given by

$$f(\lambda) \Big|_{\theta} = 4 \left[\frac{J_1(2\pi\rho\sin\theta/\lambda)}{2\pi\rho\sin\theta/\lambda} \frac{\sin(\pi l\cos\theta/\lambda)}{\pi l\cos\theta/\lambda} \right]^2, \quad (4)$$

where J_1 is the first-order Bessel function. In the forward direction ($\theta=0$), the transverse contribution vanishes, and the form factor reduces to the familiar sinc-squared function. However, for large angles or big transverse beam sizes, the transverse contribution will result in an apparent bunch-length measurement that is longer than the actual one. This

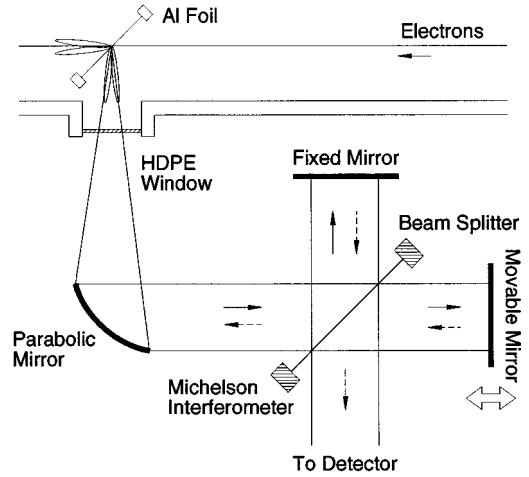


FIG. 1. Schematic diagram of a Michelson interferometer designed for bunch-length measurement.

transverse contribution can be ignored if the $2\pi\rho\sin\theta/3.83 \ll l$ condition is satisfied, which is assumed throughout this paper. Therefore good focusing to produce small transverse beam size and a reasonable angular acceptance for the detector are crucial for accurate subpicosecond bunch-length measurements.

B. Michelson interferometer

Since the spectrum of coherent transition radiation emitted by subpicosecond electron bunches is in the far-infrared regime, a far-infrared Michelson interferometer is used to measure the spectrum via optical autocorrelation, and the bunch length can be deduced from the autocorrelation measurement. A Michelson interferometer used to measure the bunch length is shown schematically in Fig. 1. It consists of a beam splitter, a fixed and a movable mirror, and a detector. When light enters the Michelson interferometer, the beam splitter splits its amplitude into two mirror arms. As these two rays are reflected from the mirrors, they are recombined at the beam splitter and sent into the detector.

An ideal beam splitter has constant amplitude reflection (R) and transmission (T) coefficients over all frequencies, which satisfy $|R|^2 = |T|^2 = \frac{1}{2}$. As shown in Fig. 1, for an incoming light pulse of electric field E with intensity proportional to $|E|^2$, the light pulse split by the beam splitter and reflected by the fixed mirror has a field amplitude of $TR E$ when it reaches the detector; on the other hand, the light pulse reflected by the movable mirror has an amplitude of RE at the detector. Note that perfect reflection on the mirrors is assumed. At zero optical path difference, the pulses completely overlap at the detector, and the total intensity reaches the maximum $|2RE|^2 = 4|RE|^2 = 2|E|^2$. All the incident energy goes into the detector. As the path difference increases but is still shorter than the bunch length, the two pulses overlap partially, and the total intensity decreases. Part of the incident energy now goes back to the source. When the path difference of two arms is larger than the bunch length, the two pulses are totally separated in time, and the resulting intensity at the detector is $2|RE|^2 = |E|^2$. Only half of the incident energy goes into the detector, while the other half goes back to the source. The intensity is

constant over all path differences greater than the bunch length and is called the *baseline*. The variation of intensity about the baseline as a function of optical path difference is defined as the *interferogram*. Therefore the width of the peak in the interferogram can be used to estimate the bunch length. For example, the bunch length is equal to the full width at half maximum (FWHM) of the interferogram for a rectangular bunch distribution; however, for a Gaussian bunch distribution, its equivalent bunch length ($\sqrt{2\pi}\sigma_z$) is about 75% of the interferogram FWHM, i.e.,

$$\frac{(\text{equivalent bunch length})}{(\text{interferogram FWHM})} = \begin{cases} 1, & \text{rectangular;} \\ 0.75, & \text{Gaussian.} \end{cases} \quad (5)$$

The interferogram is obtained by measuring the detector signal as a function of the path difference in the two arms. The intensity of the recombined radiation intensity at the detector can be expressed in the time domain with an additional time delay δ/c for the movable arm by

$$\begin{aligned} I(\delta) &\propto \int_{-\infty}^{+\infty} |TRE(t) + RTE\left(t + \frac{\delta}{c}\right)|^2 dt \\ &= 2|RT|^2 \text{Re} \int_{-\infty}^{+\infty} E(t)E^*\left(t + \frac{\delta}{c}\right) dt \\ &\quad + 2|RT|^2 \int_{-\infty}^{+\infty} |E(t)|^2 dt; \end{aligned} \quad (6)$$

alternatively, in the frequency domain an extra phase difference $e^{-i\omega\delta/c}$ is added to the radiation from the movable arm, and the intensity at the detector can be expressed by

$$\begin{aligned} I(\delta) &\propto \int_{-\infty}^{+\infty} |TR\tilde{E}(\omega) + RT\tilde{E}(\omega)e^{-i\omega\delta/c}|^2 d\omega \\ &= 2\text{Re} \int_{-\infty}^{+\infty} |RT|^2 |\tilde{E}(\omega)|^2 e^{-i\omega\delta/c} d\omega \\ &\quad + 2 \int_{-\infty}^{+\infty} |RT|^2 |\tilde{E}(\omega)|^2 d\omega, \end{aligned} \quad (7)$$

where δ is the optical path difference and c the speed of light. Equations (6) and (7) are related by the Fourier transform

$$\tilde{E}(\omega) = \frac{1}{\sqrt{2\pi}} \int_{-\infty}^{+\infty} E(t)e^{i\omega t} dt. \quad (8)$$

The baseline is defined as the intensity at $\delta \rightarrow \pm\infty$; i.e.,

$$I_\infty \propto 2|RT|^2 \int_{-\infty}^{+\infty} |E(t)|^2 dt = 2 \int_{-\infty}^{+\infty} |RT|^2 |\tilde{E}(\omega)|^2 d\omega. \quad (9)$$

By definition, the interferogram can be written

$$S(\delta) = I(\delta) - I_\infty \propto 2|RT|^2 \text{Re} \int_{-\infty}^{+\infty} E(t)E^*\left(t + \frac{\delta}{c}\right) dt \quad (10)$$

$$= 2\text{Re} \int_{-\infty}^{+\infty} |RT|^2 |\tilde{E}(\omega)|^2 e^{-i\omega\delta/c} d\omega. \quad (11)$$

Therefore, the interferogram $S(\delta)$ is the autocorrelation of the incident light pulse [cf. Eq. (10)], and its Fourier transform is the power spectrum of the pulse [cf. Eq. (11)]. Solving for $|\tilde{E}(\omega)|^2$ in Eq. (11) yields

$$|\tilde{E}(\omega)|^2 \propto \frac{1}{4\pi c|RT|^2} \int_{-\infty}^{+\infty} S(\delta)e^{i\omega\delta/c} d\delta, \quad (12)$$

where $|\tilde{E}(\omega)|^2 = |\tilde{E}(-\omega)|^2$ is used since $E(t)$ is a real function. Using Eq. (2) and the relation $I_{\text{total}}(\lambda) \propto |\tilde{E}(2\pi c/\lambda)|^2$, the bunch form factor can be obtained by

$$f(\lambda) \propto \frac{1}{N-1} \left[\frac{\int_{-\infty}^{+\infty} S(\delta)e^{i2\pi\delta/\lambda} d\delta}{4\pi c|RT|^2 N I_e(\lambda)} - 1 \right]. \quad (13)$$

Hence the interferogram contains the frequency spectrum of coherent transition radiation and can be used to derive the bunch length.

C. Beam-splitter interference effects

Suitable beam splitters for the far-infrared regime (a Mylar foil in our design) do not provide constant and equal reflectance and transmittance for all frequencies. This departure from an ideal beam splitter is caused by the interference of light reflected from both surfaces of the beam splitter, which is equivalent to thin-film interference in optics [8]. The total amplitude reflection coefficient for a Mylar foil of thickness t and refractive index n mounted at a 45° angle to the direction of incoming light is given by [9]

$$R = -r \frac{1 - e^{i\phi}}{1 - r^2 e^{i\phi}}, \quad (14)$$

where r is the amplitude reflection coefficient of the air-to-Mylar interface at an incident angle of 45° , and ϕ defined as $4\pi t \sigma \sqrt{(2n^2 - 1)}/2$ at wave number $\sigma = 1/\lambda$ [10]. The total amplitude transmission coefficient for the same condition is

$$T = (1 - r^2) \frac{e^{i\phi/2}}{1 - r^2 e^{i\phi}}. \quad (15)$$

No absorption in the foil is assumed, and the refractive index is assumed to be constant ($n = 1.85$) over all frequencies [10]. The phase difference between R and T is $\pi/2$ at any frequency. With this, energy conservation in the interferometer can be proved [9].

The efficiency of the beam splitter defined as $|RT|^2$ is shown in Fig. 2 for some typical thicknesses. Unlike the ideal beam splitter, the efficiency is not constant over all frequencies and becomes zero at certain frequencies where light reflected from both surfaces of the beam splitter interferes destructively. Equations in the time domain, such as Eq. (6), are no longer valid for the case of varying efficiency

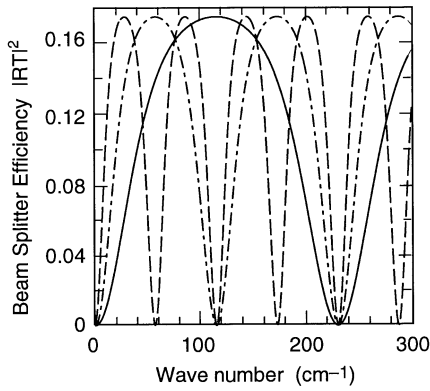


FIG. 2. The efficiency of the Mylar beam splitter as a function of frequency for different thicknesses: 12.7 (solid), 25.4 (dash-dotted), and 50.8 μm (dashed line). The incident light is assumed to be unpolarized.

and need to be replaced by appropriate convolution integrals; however, equations in the frequency domain such as Eq. (7) still hold. The width of the interferogram cannot be directly used for bunch-length estimation unless interference effects on the interferogram are included.

D. Bunch-length analysis

Although the interference effects on the interferogram caused by the complex reflection and transmission coefficients of the beam splitter do not seem to have simple analytical forms, these effects can be studied numerically for known bunch distributions, and the bunch length can be estimated from the study. Both Gaussian and rectangular bunch distributions are currently used in this study. While most real bunch distributions are neither Gaussian nor rectangular, the bunch lengths estimated from the two distributions will give reasonable bounds for the real one.

The beam-splitter affected interferogram can be obtained numerically by using the spectrum of a known bunch distribution and Eqs. (7), (14), and (15). Some numerical results of the beam-splitter interference effects for a rectangular bunch distribution are shown in Fig. 3. For an ideal beam splitter, the interferogram is non-negative and has the expected triangular peak with its FWHM equal to the bunch length [cf. Fig. 3(a)]. For Mylar beam splitters, negative valleys appear in the interferograms, which are due to suppression of the low frequency area by the first zero of the beam-splitter efficiency. These valleys move closer to the main peak as the beam-splitter thickness (t) decreases [cf. Figs. 3(b)–3(d)]. For very thin beam splitters [thinner than about half the equivalent bunch length (l_b)], they merge with the main peak and make the peak narrower [cf. Fig. 3(d)]. The effects are similar for a Gaussian distribution. Detailed results on how the FWHM values in the interferogram change with the equivalent bunch length for both Gaussian and rectangular distributions are shown in Fig. 4 for some Mylar beam-splitter thicknesses. The raggedness of the lines for rectangular distribution is due to the high-frequency lobes of the sinc function. On the other hand, Gaussian distribution has smoother variation in the high frequency area, and the resulting slopes of the lines are smoother. When the equivalent bunch length is shorter than about twice the beam-

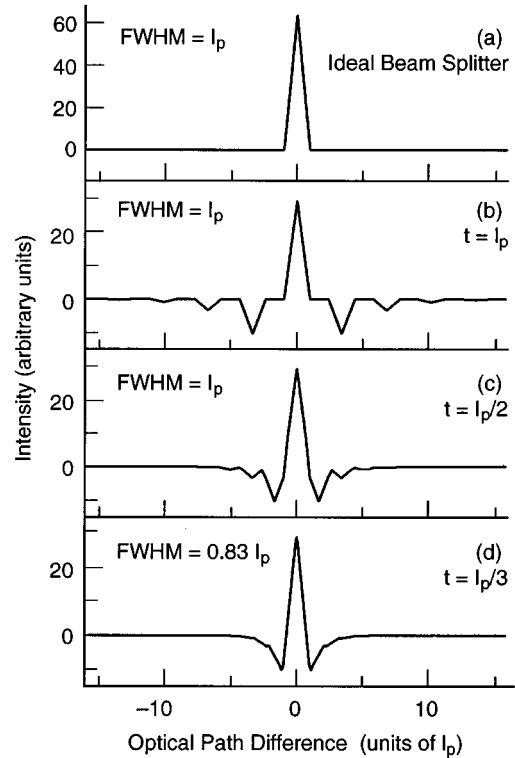


FIG. 3. The simulation of the beam-splitter interference effects for a rectangular bunch distribution with different beam splitters. The interferograms for (a) an ideal beam splitter and Mylar beam splitters of thicknesses (t) (b) equal to, (c) half, and (d) one third of the bunch length (l_b) are shown.

splitter thickness, the valleys in the interferogram are separated from the main peak, and the relation between the interferogram FWHM and the equivalent bunch length is the same as that for the ideal beam splitter in Eq. (5). The slopes of the lines become unity for rectangular distribution and 1/0.75 for a Gaussian. As the equivalent bunch length becomes greater than about twice the beam-splitter thickness, the valleys cut into the main peak and narrow its width. This

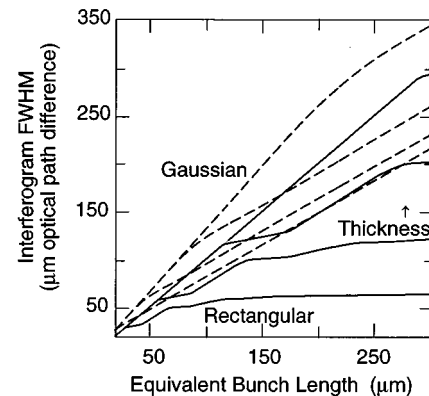


FIG. 4. Interferogram FWHM's as functions of equivalent bunch lengths of both Gaussian (dotted lines) and rectangular (solid lines) bunch distributions for different Mylar beam-splitter thicknesses: 12.7, 25.4, 50.8, and 127 μm . Within the same distribution, the lines are shown from the bottom to the top in increasing order of thickness. The FWHM's are in terms of optical path difference.

peak-narrowing effect reduces the slopes of the lines for rectangular distribution at longer bunch length and, hence, makes the interferogram width less sensitive to the bunch-length change and increases the uncertainty of estimated bunch length. Therefore a beam splitter of suitable thickness is important for effective bunch-length measurement. As indicated in Fig. 4, thicker beam splitters are more preferable for bunch-length measurement. Once the beam splitter is chosen, the bunch length can be derived from the measured interferogram width with the help of Fig. 4.

III. EXPERIMENTAL SETUP

For this experiment, the SUNSHINE facility was operated to produce 1- μ s-long electron macropulses at 10 Hz containing a train of about 3 000 electron bunches at an energy of 30 MeV. Each bunch had about 3.5×10^7 electrons. The bunch length is to be determined by this autocorrelation method. As shown in Fig. 1, transition radiation is generated when the electrons pass through a 25.4- μ m-thick Al foil. The foil supported by a copper ring is oriented at a 45° angle to the beam direction so that backward transition radiation is emitted in the direction normal to the beam path and can easily be extracted from the evacuated beam line into air via a 1-mm-thick high-density polyethylene (HDPE) window of 19 mm diameter. Since backward transition radiation is emitted at the Al surface, the focal point of an off-axis paraboloidal mirror is aligned with this surface to convert the divergent radiation into parallel light without introducing extra optical path difference to the extracted light pulse. The parallel light then enters a far-infrared Michelson interferometer.

The interferometer consists of a Mylar beam splitter supported by an Al ring, a fixed and a movable first-surface mirror, and a room-temperature detector. The beam splitter is mounted at a 45° angle to the direction of incident parallel light. The movable mirror is moved by a linear actuator via a 486-based personal computer. The detector consists of a Moletron P1-65 LiTaO₃ pyroelectric bolometer of 5 mm diameter and a preamplifier. Its bolometer has a wide spectral response from millimeter waves to ultraviolet rays. This detector is designed to measure the integrated radiation energy from each 1- μ s macropulse and is attached to a copper light cone [11], which collects the light into the detector. The detector signal is digitized into the computer. With the computer interfaces, the autocorrelation measurements are performed automatically through the program under the LabVIEW control environment implemented on the computer.

IV. RESULTS AND DISCUSSION

It has been confirmed that backward transition radiation emitted by the electron pulses generated at SUNSHINE is coherent in the previous experiment [3]. Therefore the spectrum measured by the autocorrelation method contains the information of the bunch distribution and can be used to derive the bunch length. By measuring the detector signal as a function of the position of the movable mirror via the computer program, the interferograms of 2.2 mm long with 5 μ m mirror step size are measured for four different Mylar beam-splitter thicknesses and shown in Fig. 5. This 5 μ m mirror step size corresponding to a 33 fs time resolution is

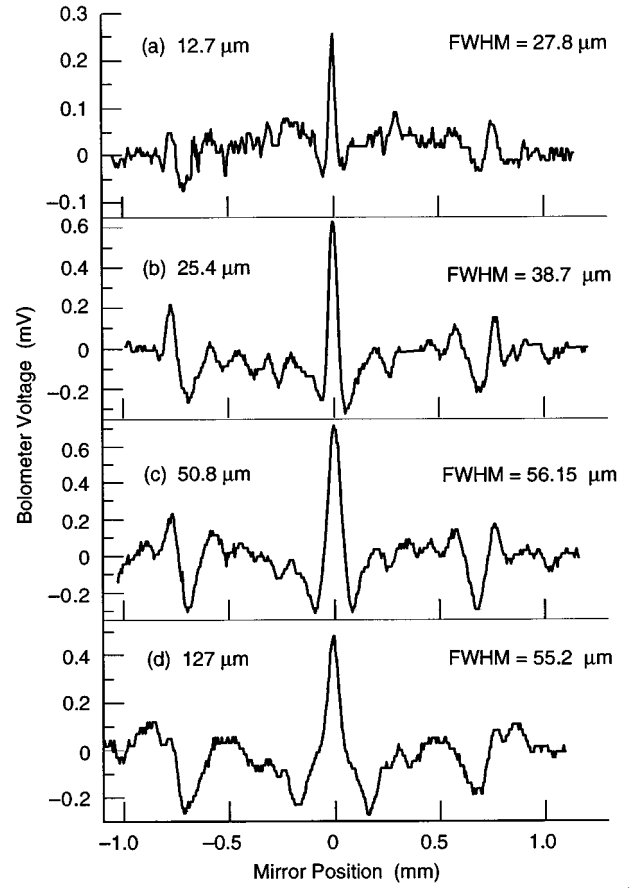


FIG. 5. Interferograms of 2.2 mm long with 5 μ m mirror step size for different Mylar beam-splitter thicknesses: (a) 12.7, (b) 25.4, (c) 50.8, and (d) 127 μ m. The FWHM's of the main peaks are measured in terms of mirror movement. The corresponding widths in terms of optical path difference are twice this movement.

good enough for the experiments; however finer resolution can still be achieved by the actuator. The beam parameters are kept the same when different beam splitters are used. The valleys around the main peak are separated farther apart as the beam-splitter thickness increases. This widens the main peak [cf. Figs. 5(a)–5(c)] until the valleys are out of the peak [cf. Figs. 5(c), 5(d)]. The base of the peak can even be seen in Fig. 5(d). In the figure, the FWHM's of the main peaks are measured in terms of mirror movement. The corresponding widths in terms of optical path difference are twice this movement. These measured interferogram FWHM's and the estimated equivalent bunch lengths deduced from Fig. 4 for Gaussian and rectangular distributions are shown in Table I. The estimated bunch lengths provide intervals for the real bunch length. As the beam-splitter thickness increases from 12.7 to 50.8 μ m, the interval narrows down, which indicates the estimation gets better for a thicker beam splitter. Additionally, the intervals stay the same for 50.8 and 127 μ m beam splitters and agree with the estimation made from Eq. (5) for the ideal beam splitter. It is also worth noticing that the estimated intervals are consistent over a tenfold change in the beam-splitter thickness. The estimated equivalent bunch length is about 100 μ m long, which corresponds to a rms bunch length of $\sigma_z \approx 43$ μ m or $\sigma_t \approx 142$ fs.

For linear accelerators, using a solid metal foil to generate

TABLE I. Measured interferogram FWHM's in terms of optical path difference (OPD) for different beam-splitter thicknesses and the corresponding estimated equivalent bunch lengths deduced from Fig. 4 for Gaussian and rectangular distributions.

Beam splitter thickness (μm)	Interferogram FWHM OPD (μm)	Estimated equivalent bunch length (μm)	
		Gaussian	Rectangular
12.7	55.6	60.8	100.6
25.4	77.4	72.8	103.2
50.8	112.3	86.9	111.0
127.0	110.4	83.1	109.1

coherent transition radiation for the interferometer does not seem to cause a problem, although it generally destroys the electron-beam quality. However such a destructive procedure cannot be applied to circular accelerators. Nondestructive methods (such as using a bending magnet to generate coherent synchrotron radiation [12] or using a metal foil with a center hole to generate coherent transition radiation) are suitable for this application, despite the fact that the measured spectrum has to be corrected for the frequency dependence of these generating methods [i.e., $I_e(\lambda)$ in Eq. (2)] in order to extract bunch information $f(\lambda)$.

In principle, the measured spectral information can be used to reconstruct the bunch distribution and give a better bunch-length measurement. However there are some practical difficulties in reconstructing the electron distribution for this experiment. First, the spectrum is contaminated by water absorption lines [4,5] because the interferometer is not protected from humidity. These lines are hard to remove, and their effects on the reconstructed distribution are not clear. Secondly, the zeros of the beam-splitter efficiency produce artificial peaks when the spectrum is numerically corrected for the beam-splitter interference effects [4,5]. Unfortunately, in the presence of measurement noises, these peaks are also not easy to remove. Finally, there are infinite distributions which give the same autocorrelation even if the constraints for non-negative and real electron distribution are employed. Although one-dimensional phase-retrieval methods have been suggested for this reconstruction problem

[12,13], they cannot guarantee the uniqueness of the solution, not to mention the immunity against noise in data. Structures generated by these reconstruction methods need to be verified as to whether they are real bunch structures or the artifacts produced by the methods.

V. CONCLUSION

In conclusion, an alternative frequency-resolved bunch-length measuring method specialized for subpicosecond electron pulses has been developed at the SUNSHINE facility. This method measures the autocorrelation of coherent transition radiation emitted at wavelengths longer than or equal to the bunch length via a far-infrared Michelson interferometer. The bunch length can be derived from the interferogram with special consideration of interference effects in the beam splitter. Measurements have verified this method by showing consistent results over a broad range of beam-splitter thicknesses. Based on a low-cost, easy-to-operate, compact, and transportable Michelson interferometer, this autocorrelation method demonstrates subpicosecond resolving power beyond the reach of existing time-resolved methods.

ACKNOWLEDGMENTS

This work was supported in part by Department of Energy Contract No. DE-AC03-76F00515.

-
- [1] R. L. Fork, B. I. Greene, and C. V. Shank, *Appl. Phys. Lett.* **38**, 671 (1981).
- [2] W. Barry, (unpublished); CEBAF Report No. PR-91-012, 1991 (unpublished).
- [3] P. Kung, H.-C. Lihn, D. Bocek, and H. Wiedemann, *Proc. Soc. Photo Opt. Instrum. Eng.* **2118**, 191 (1994).
- [4] P. Kung, H.-C. Lihn, D. Bocek, and H. Wiedemann, *Phys. Rev. Lett.* **73**, 967 (1994).
- [5] H.-C. Lihn, P. Kung, D. Bocek, and H. Wiedemann, *Beam Instrumentation Workshop*, edited by G. H. Mackenzie, B. Rawnsley, and J. Thomson, AIP Conf. Proc. No. 333, (AIP, New York, 1995), p. 231.
- [6] I. M. Frank and V. L. Ginsburg, *J. Phys. (Moscow)* **9**, 353 (1945); M. L. Ter-Mikaelian, *High-energy Electromagnetic Processes in Condensed Media* (Wiley-Interscience, New York, 1972), Chap. 4.
- [7] H. Motz, *J. Appl. Phys.* **22**, 527 (1951); J. S. Nodvic and D. S. Saxon, *Phys. Rev.* **96**, 180 (1954).
- [8] E. Hecht and A. Zajac, *Optics* (Addison-Wesley, Reading, Massachusetts, 1974), Sec. 9.7.
- [9] G. W. Chantry, *Submillimetre Spectroscopy* (Academic, London, 1971), Ap. A.
- [10] R. J. Bell, *Introductory Fourier Transform Spectroscopy* (Academic, London, 1972), Chap. 9.
- [11] D. E. Williamson, *J. Opt. Soc. Am.* **42**, 712 (1952).
- [12] R. Lai, U. Happek, and J. Sievers, *Phys. Rev. E* **50**, R4294 (1994).
- [13] J. R. Fienup, *Opt. Lett.* **3**, 27 (1978).